INTERNATIONAL JOURNAL FOR NUMERICAL METHODS IN ENGINEERING, VOL. 1, 101–122 (1969)

# A REFINED TRIANGULAR PLATE BENDING FINITE ELEMENT

KOLBEIN BELL
*Division of Structural Mechanics,*
*The Technical University of Norway, Trondheim, Norway*

## SUMMARY

The derivation of the stiffness matrix for a refined, fully compatible triangular plate bending finite element is presented. The Kirchhoff plate bending theory is assumed. Six parameters or degrees of freedom are introduced at each of the three corner nodes resulting in an 18 degree of freedom element. This refined element is found to give better results for displacements and particularly for internal moments than any plate bending element, regardless of shape, previously reported in the literature.

## INTRODUCTION

The finite element method originally developed by Turner and others[1] has proved to be a convenient and powerful technique for the approximate analysis of problems of continuum mechanics. A comprehensive presentation of the method and its many applications has been given by Zienkiewicz.[2]

The finite element concept is essentially a generalization of standard structural procedures to two- and three-dimensional structures. In a plate bending problem the plate structure is idealized as an assemblage of a finite number of appropriately shaped elements interconnected at a finite number of nodal points or nodes. As in the case of simple structures, the analysis involves the evaluation of the relationship between element nodal displacements and corresponding element nodal forces. This relationship is conveniently expressed in terms of the element stiffness matrix, the evaluation of which is the key step of the finite element displacement method.

Of the various shapes of plate bending finite elements the triangle is the most attractive because it makes it possible to treat plates with irregular boundaries. With triangular elements it is easy to vary the element size in the vicinity of stress concentrations, and it is possible to approximate the geometry of arbitrary doubly curved shell structures.

Many investigators have concerned themselves with the problem of determining suitable stiffness characteristics for triangular plate bending elements. An excellent summary has been given by Clough and Tocher[3] who also present the stiffness matrix for a compatible 9 degree of freedom element. Zienkiewicz and others[4] using a somewhat different approach also construct stiffness matrices for compatible triangular plate bending elements with 9 degrees of freedom. With these elements the displacements can in most cases be determined with satisfactory accuracy when fine mesh systems are used. However, the accuracy of the results obtained for the internal moments is more doubtful.

Hellan[5] and Herrmann[6] have developed a simplified method, which is not a stiffness method, for the analysis of plate bending by triangular elements. This method appears to give reasonably good results for fine mesh idealizations.

Results obtained with a refined rectangular plate bending element,[7] as well as those obtained with a refined triangular plane stress element,[8,9] seem to indicate that there is much to be said for more refined element stiffness matrices.

*Received 15 June 1968*

The purpose of this paper is to present the development of the stiffness matrix for a refined triangular plate bending element which ensures displacement and slope compatibility along the edges of adjacent elements. In addition to the deflection and the two rotation components, the three curvature components are introduced as parameters at each of the three corner nodes, thus resulting in an 18 degree of freedom element. This element is obtained by eliminating three degrees of freedom associated with three midside nodes of a 21 degree of freedom element which in turn is based on a displacement field assumed as a complete fifth degree polynomial in $x$ and $y$.

## THIN PLATE THEORY

The notation and sign conventions used in this paper are shown in Figure 1, where all forces and moments shown act in the positive direction. It should be noted that the lateral displacement $w$ is taken as positive in the downward direction, i.e. in the direction of negative $z$.

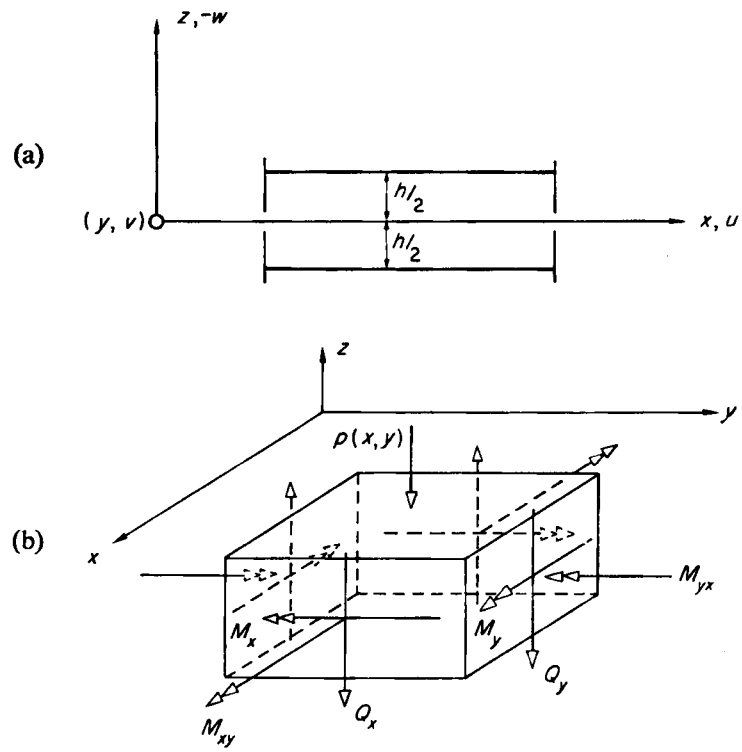


Figure 1. (a) Plate coordinate system and displacement notation;
(b) Notation for stress resultants and loading

The classical theory of thin elastic plates (Kirchhoff's theory) is well known[10] and need not be presented in any detail. It is based on assumptions which imply that the deformed state of the plate can be described entirely by the lateral displacement $w$ of the middle surface.

Introducing the notation

$$\frac{\partial w}{\partial x} = w_{,x}\,, \quad \frac{\partial^2 w}{\partial x^2} = w_{,xx}\,, \quad \frac{\partial^2 w}{\partial x \partial y} = w_{,xy} \quad \text{etc.}$$

the moment-curvature relation may be expressed as

$$\begin{Bmatrix} M_x \\ M_y \\ M_{xy} \end{Bmatrix} = -D \begin{bmatrix} 1 & \nu & 0 \\ \nu & 1 & 0 \\ 0 & 0 & \dfrac{1-\nu}{2} \end{bmatrix} \begin{Bmatrix} w_{,xx} \\ w_{,yy} \\ 2w_{,xy} \end{Bmatrix} \tag{1a}$$

where

$$D = \frac{Eh^3}{12(1-\nu^2)}$$

is the flexural rigidity of the plate. $E$ is the modulus of elasticity and $\nu$ is Poisson's ratio.

With matrix symbols* equation (1a) may be written as

$$\mathbf{m} = -\mathbf{D}\mathbf{c} \tag{1b}$$

## ELEMENT STIFFNESS ANALYSIS

The element stiffness relation may be expressed as

$$\mathbf{S} = \mathbf{k}\mathbf{v} \tag{2}$$

where $\mathbf{k}$ is the element stiffness matrix. The vector $\mathbf{v}$ contains a set of selected displacement parameters defined at the nodal points of the element (they may be regarded as kinematic degrees of freedom), and the vector $\mathbf{S}$ contains the nodal forces corresponding with $\mathbf{v}$.

Methods of calculating element stiffness matrices have been discussed by a number of authors.[11,12] However, in order to establish the notation used in this paper and also for the sake of completeness, an outline of the standard element stiffness analysis procedure will be presented.

Assuming the Kirchhoff plate bending theory to be applicable the deformed state of the plate element is completely defined by the lateral displacement, which in terms of assumed displacement patterns may be expressed as

$$w(x,y) = q_1\phi_1 + q_2\phi_2 + q_3\phi_3 + \ldots$$

or

$$w(x,y) = \langle \phi_1\ \phi_2 \ldots \rangle \begin{Bmatrix} q_1 \\ q_2 \\ \vdots \\ \vdots \end{Bmatrix} = \boldsymbol{\phi}^T\mathbf{q} \tag{3}$$

where $\phi_i = \phi_i(x, y)$ $(i = 1, 2, 3, \ldots)$ are assumed displacement patterns having amplitudes $q_i$ which may be regarded as generalized displacement parameters. The superscript $T$ denotes the transpose of a vector or a matrix.

---

* Vectors and matrices are represented by bold-type characters.

The curvatures, defining the element strains, are

$$\mathbf{c} = \begin{Bmatrix} w_{,xx} \\ w_{,yy} \\ 2w_{,xy} \end{Bmatrix} = \mathbf{P}\,\mathbf{q} \tag{4}$$

where the matrix $\mathbf{P}$ is obtained by appropriate differentiation of $\phi$.

The internal moments are found by substituting equation (4) into equation (1b).

$$\mathbf{m} = -\mathbf{DPq} \tag{5}$$

Let the element be subjected to a virtual displacement field

$$\tilde{w}(x,y) = \boldsymbol{\phi}^T\tilde{\mathbf{q}}$$

Equating the external and the internal work done during this displacement yields

$$\tilde{\mathbf{q}}^T\mathbf{Q} = -\int_A \tilde{\mathbf{c}}^T\mathbf{m}\,dA$$

or, by use of equations (4) and (5),

$$\tilde{\mathbf{q}}^T\mathbf{Q} = \tilde{\mathbf{q}}^T\int_A \mathbf{P}^T\mathbf{DP}\,dA\,\mathbf{q}$$

where the vector $\mathbf{Q}$ contains a set of generalized forces corresponding with the displacements $\mathbf{q}$. A denotes the area of the element. The above equation is valid for any $\tilde{\mathbf{q}}$. Hence

$$\mathbf{Q} = \mathbf{k}_q\mathbf{q} \tag{6}$$

in which

$$\mathbf{k}_q = \int_A \mathbf{P}^T\mathbf{DP}\,dA \tag{7}$$

is the generalized element stiffness matrix.

The relationship between the nodal displacement parameters and the generalized displacements may be written as

$$\mathbf{v} = \mathbf{Aq} \tag{8}$$

where the matrix $\mathbf{A}$ is obtained by merely substituting the coordinates of the nodal points into the displacement functions (equation 3) and their appropriate derivatives.

From equation (8)

$$\mathbf{q} = \mathbf{Bv} \tag{9}$$

where

$$\mathbf{B} = \mathbf{A}^{-1} \tag{10}$$

The desired element stiffness matrix is now defined by the following transformation

$$\mathbf{k} = \mathbf{B}^T\mathbf{k}_q\mathbf{B} \tag{11}$$

As the matrix **D** is a symmetrical matrix (equation 1a) it follows from equations (7) and (11) that **k** is a symmetrical matrix.

From equation (10) it follows that **A** must be a square, non-singular matrix. This implies that the number of assumed displacement patterns must be equal to the number of nodal displacement parameters (number of nodal degrees of freedom), and also that the functions $\phi_i$ ($i = 1, 2, 3 \ldots$) are linearly independent of each other.

It is evident that the accuracy of the finite element solution is directly dependent upon the extent to which the assumed displacement patterns or functions can approximate the true distortions of the plate, and the deformations will not necessarily converge to the correct values as the element mesh size is successively reduced unless the displacement functions are properly chosen.

The basic requirement which the assumed displacement functions must satisfy is what might be called the completeness criterion, i.e. they must be capable of describing all possible rigid body displacements of the elements as well as representing constant strain conditions (constant curvatures) within the elements.[2] In the case of polynomial displacement functions the completeness criterion requires a complete quadratic polynomial to be present in the assumed expression for $w$. If the assumed displacement functions in addition to satisfying the completeness criterion also provide for complete displacement and slope compatibility, i.e. single-valued deflection and slopes within the elements as well as along the boundaries between adjacent elements, the finite element solution will provide a lower bound to the strain energy of the system and the results will converge toward the true state of deformation as the mesh size is reduced.[1,2,3]

The finite element solution should be invariant, i.e. independent of the position of the external (global) reference system. The displacement functions should therefore be independent of the orientation of the element with respect to the coordinate axes to which the functions are referred.

## COORDINATE SYSTEMS AND INTEGRATION FORMULAE FOR A PLANE TRIANGLE

In recent works dealing with triangular finite elements, whether plate bending or plane stress elements, the so-called area or triangular coordinates have been extensively used, partly in order to avoid the two major difficulties encountered in cartesian coordinates, which are

1. Derivation in cartesian coordinates leads very often to a lack of invariance.

2. Evaluation of the integral in equation (7) for all elements of the generalized stiffness matrix can be an extremely tedious operation in cartesian coordinates.

These difficulties can, however, be overcome without introducing a different coordinate system. Invariance is automatically satisfied if a complete polynomial expansion in $x$ and $y$ is used to describe the lateral displacement, and it will be shown that very simple integration formulae can be found by making use of the corresponding formulae in area coordinates.

### *Cartesian coordinates*

A plane triangle 1-2-3 lies in the $\bar{x}$–$\bar{y}$ plane of a global cartesian coordinate system $\bar{x}$, $\bar{y}$, $\bar{z}$ as shown in Figure 2. The coordinates of the corners are $(\bar{x}_1, \bar{y}_1)$, $(\bar{x}_2, \bar{y}_2)$ and $(\bar{x}_3, \bar{y}_3)$.

A 'local global' cartesian system $x$, $y$, $z$ is defined with the axes parallel to the corresponding global axes $\bar{x}$, $\bar{y}$, $\bar{z}$ and with the origin located at the centroid of the triangle area.

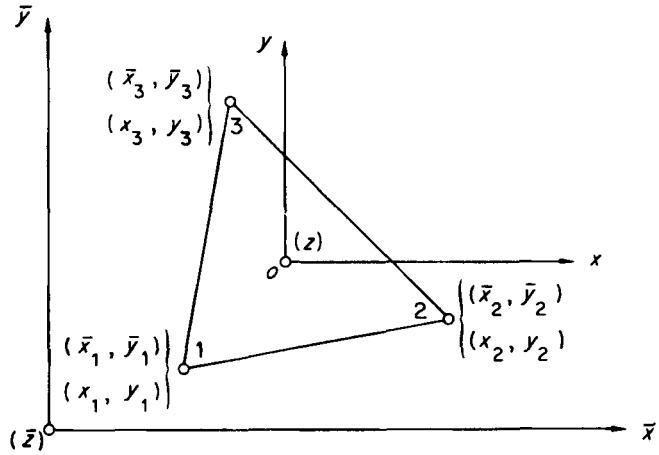


Figure 2. Global and local cartesian system

The global coordinates of the centroid are

$$\left.\begin{aligned} \bar{x}_0 &= \frac{1}{3}(\bar{x}_1 + \bar{x}_2 + \bar{x}_3) \\ \bar{y}_0 &= \frac{1}{3}(\bar{y}_1 + \bar{y}_2 + \bar{y}_3) \end{aligned}\right\} \tag{12}$$

The local coordinates of the triangle corners may be expressed in terms of the global coordinates as

$$\left.\begin{aligned} x_i &= \bar{x}_i - \bar{x}_0 \\ y_i &= \bar{y}_i - \bar{y}_0 \end{aligned}\right\} \qquad i = 1, 2, 3 \tag{13}$$

Hence

$$\left.\begin{aligned} x_1 + x_2 + x_3 &= 0 \\ y_1 + y_2 + y_3 &= 0 \end{aligned}\right\} \tag{14}$$

The area of the triangle may be expressed in terms of the corner coordinates by the following third-order determinant

$$A = \tfrac{1}{2}\begin{vmatrix} 1 & x_1 & y_1 \\ 1 & x_2 & y_2 \\ 1 & x_3 & y_3 \end{vmatrix} \tag{15}$$

*Area coordinates*

Any point $P(\bar{x}, \bar{y})$ within the triangle 1-2-3 divides it into three sub-triangles as shown in Figure 3. Let $A_1$, $A_2$ and $A_3$ be the areas of these sub-triangles, the index designating the opposite corner number.

The three area coordinates of $P$ are defined as

$$\omega_i = \frac{A_i}{A} \qquad i = 1, 2, 3 \tag{16}$$

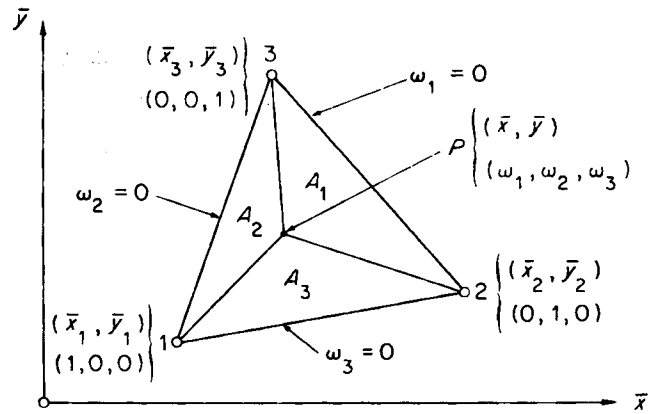


Figure 3. Area coordinates

where $A = A_1 + A_2 + A_3$ is the total area of the triangle. It follows that

$$\omega_1 + \omega_2 + \omega_3 = 1 \tag{17}$$

The equation $\omega_i = \text{constant}$ represents a line parallel to the side opposite corner '$i$'. The corner '$i$' has the area coordinates $\omega_i = 1$ and $\omega_j = \omega_k = 0$ $(i \neq j \neq k)$.

*Relationship between cartesian and area coordinates*

The cartesian coordinates are related to the area coordinates by the following matrix equation,

$$\begin{Bmatrix} 1 \\ x \\ y \end{Bmatrix} = \begin{bmatrix} 1 & 1 & 1 \\ x_1 & x_2 & x_3 \\ y_1 & y_2 & y_3 \end{bmatrix} \begin{Bmatrix} \omega_1 \\ \omega_2 \\ \omega_3 \end{Bmatrix} \tag{18}$$

where $x$ and $y$ are the cartesian coordinates and $\omega_1$, $\omega_2$ and $\omega_3$ the area coordinates of any point $P$ within the triangle or on the triangle sides. $x_i$, $y_i$ $(i = 1, 2, 3)$ are the coordinates of the triangle corners. Equation (18) is valid for any position of the cartesian coordinates system.

*Integration formulae*

The integration over the triangle area of polynomial terms in area coordinates is independent of the shape of the triangle and may be expressed as a fraction of the area, or

$$\int_A \omega_i^{m_i} \omega_j^{m_j} \omega_k^{m_k} \, dA = \rho A \tag{19}$$

where the indices $i$, $j$, and $k$ represent any permutation of 1, 2 and 3, and where the factor $\rho$ is found.[9,13]

$$\rho = 2 \frac{(m_i)!(m_j)!(m_k)!}{(m_i + m_j + m_k + 2)!} \tag{20}$$

Consider the local cartesian coordinate system $x$, $y$ with the origin located at the centroid of the triangle, Figure 2, and let

$$P_{rs} = \int_A x^r y^s \, dA \tag{21}$$

From equation (18) it follows that

$$x = x_1\omega_1 + x_2\omega_2 + x_3\omega_3$$

$$y = y_1\omega_1 + y_2\omega_2 + y_3\omega_3$$

Substituting gives

$$P_{rs} = \int_A (x_1\omega_1 + x_2\omega_2 + x_3\omega_3)^r (y_1\omega_1 + y_2\omega_2 + y_3\omega_3)^s \, dA \tag{22}$$

For given values of $r$ and $s$ the right-hand side of this equation may be evaluated by the use of equations (19), (20) and (14). The evaluation of $P_{rs}$ is straightforward but tedious and will not be shown here. Formulae for $P_{rs}$ for orders $n = r + s = 1$ to 6 are listed in Table I. It is seen that these formulae are extremely simple for polynomial terms up to and including the 5th order. Unfortunately the formulae for the 6th order terms cannot be expressed in the same simple form. This inconvenience is, however, hardly noticeable when the formulae are programmed for a digital computer.

Table I. Integration Formulae for a Triangle

| Order $n = r + s$ | $P_{rs} = \int_A x^r y^s \, dA$ |
|---|---|
| 1 | $P_{rs} = 0$ |
| 2 | $P_{rs} = \frac{A}{12}(x_1^r y_1^s + x_2^r y_2^s + x_3^r y_3^s)$ |
| 3 | $P_{rs} = \frac{A}{30}(x_1^r y_1^s + x_2^r y_2^s + x_3^r y_3^s)$ |
| 4 | $P_{rs} = \frac{A}{30}(x_1^r y_1^s + x_2^r y_2^s + x_3^r y_3^s)$ |
| 5 | $P_{rs} = \frac{2A}{105}(x_1^r y_1^s + x_2^r y_2^s + x_3^r y_3^s)$ |
| | $P_{60} = \frac{15}{14A} P_{40} P_{20} + \frac{A}{84} \sum_{i=1}^{3} x_i$ |
| | $P_{51} = \frac{15}{14A}(2P_{40}P_{11} + 5P_{30}P_{21} + 2P_{20}P_{31}) - \frac{A}{168} \sum_{i=1}^{3} x_i^5 y_i$ |
| 6 | $P_{42} = \frac{1}{14A}(6P_{40}P_{02} + 24P_{20}P_{22} + 30P_{30}P_{12} + 48P_{31}P_{11} + 75P_{21}^2) - \frac{11A}{840} \sum_{i=1}^{3} x_i^4 y_i^2$ |
| | $P_{33} = \frac{1}{28A}(25P_{30}P_{03} + 225P_{21}P_{12} + 36P_{20}P_{13} + 36P_{02}P_{31} + 108P_{11}P_{22}) - \frac{A}{56} \sum_{i=1}^{3} x_i^3 y_i^3$ |
| | $P_{24}$, $P_{15}$, and $P_{06}$ are found by interchanging $x$ and $y$ in the expressions for $P_{42}$, $P_{51}$ and $P_{60}$ respectively. |

Note. $x$ and $y$ refer to a cartesian coordinate system with the origin located at the centroid of the triangle.

It should be noted that the formulae would become considerably more complicated for a different position of the coordinate system.

## REFINED ELEMENT STIFFNESS MATRIX

The refined element is based on a set of assumed displacement functions which form a complete 5th order polynomial expansion in $x$ and $y$. This expansion contains the following 21 terms:

$$
\begin{array}{ccccccc}
 & & & 1 & & & \\
 & & & x & y & & \\
 & & x^2 & xy & y^2 & & \\
 & x^3 & x^2y & xy^2 & y^3 & & \\
 x^4 & x^3y & x^2y^2 & xy^3 & y^4 & & \\
x^5 & x^4y & x^3y^2 & x^2y^3 & xy^4 & y^5 &
\end{array}
$$

Consequently the element must have 21 degrees of nodal point freedom. A nodal point system as shown in Figure 4 is chosen.

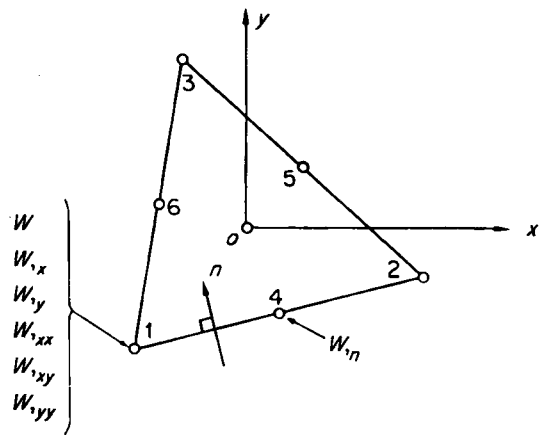


Figure 4. Nodal point system and nodal parameters

In addition to the deflection $w$ and the slopes $w_{,x}$ and $w_{,y}$ the three curvatures $w_{,xx}$, $w_{,xy}$ and $w_{,yy}$ have been introduced as parameters at each of the three corner nodes (*1*, 2, 3). This gives a total of eighteen nodal parameters or degrees of freedom, and the remaining three are the edge normal slope $w_{,n}$ at each of three mid-side nodes (4, 5, 6). These side nodes, necessary at this stage, are undesirable and will be eliminated later.

The assumed displacement functions together with the selected nodal parameters provide for displacement as well as slope compatibility along the boundaries between adjacent elements. Consider for instance two elements with a common edge having an arbitrary direction $t$. The displacement $w$ describes a quintic curve along the edge, and the edge normal slope $w_{,n}$ follows a quartic curve. The nodal parameters, which are common to both elements, provide for six 'boundary conditions' for $w$, three ($w$, $w_{,t}$ and $w_{,tt}$) at each end node. The displacement $w$ along the edge is therefore the same for both elements as a quintic curve is uniquely defined by six constants. For the edge normal slope $w_{,n}$ the nodal parameters provide for five 'boundary conditions', two ($w_{,n}$ and $w_{,nt}$) at each end node and one ($w_{,n}$) at the midside node, which is sufficient to completely define a quartic curve.

In addition to complete displacement and slope compatibility being obtained, the curvatures and consequently the internal moments are continuous between elements at the corner nodes if the thickness is continuous.

Following the standard element stiffness analysis procedure, equation (3) becomes

$$w(x,y) = \langle 1 \;\; x \;\; y \;\; x^2 \ldots x^2y^3 \;\; xy^4 \;\; y^5 \rangle \begin{Bmatrix} q_1 \\ \vdots \\ q_{21} \end{Bmatrix} = \boldsymbol{\phi}_{21}^T \mathbf{q}_{21} \tag{23}$$

where $x$ and $y$ refer to a 'local global' coordinate system with the origin at the centroid of the element, as in Figure 4. It is evident that the completeness criterion is satisfied.

The matrix $\mathbf{P}$ of equation (4) is

$$\mathbf{P}_{21} = \begin{bmatrix} 0 & 0 & 0 & 2 \ldots & 2y^3 & 0 & 0 \\ 0 & 0 & 0 & 0 \ldots & 6x^2y & 12xy^2 & 20y^3 \\ 0 & 0 & 0 & 0 \ldots & 12xy^2 & 8y^3 & 0 \end{bmatrix} \tag{24}$$

The generalized element stiffness matrix is defined by equation (7) as

$$\mathbf{k}_{q21} = \int_A [\mathbf{P}_{21}^T \mathbf{D} \, \mathbf{P}_{21}] \, dA \tag{25}$$

The integration is carried out by integrating each element of the matrix $[\mathbf{P}_{21}^T \, \mathbf{D} \, \mathbf{P}_{21}]$. With the formulae in Table I this is a straightforward operation, and explicit expressions for all elements of $\mathbf{k}_{q21}$ are easily found. The expressions for some typical elements of the generalized stiffness matrix read

$$(k_{q21})_{4\ 13} = (4P_{02} + 4\nu P_{20})D$$

$$(k_{q21})_{8\ 18} = [12P_{13} + (24 - 20\nu)P_{31}]D$$

$$(k_{q21})_{21\ 21} = 400P_{06}D$$

where the indices $i$ and $j$ of $(k_{q21})_{ij}$ denote row and column number respectively. There are altogether 153 non-zero elements on and above the main diagonal of $\mathbf{k}_{q21}$.

Equation (8) becomes

$$\mathbf{v}_{21} = \mathbf{A}_{21} \mathbf{q}_{21} \tag{26}$$

The nodal displacement parameters are listed in the vector $\mathbf{v}_{21}$ as

$$\mathbf{v}_{21} = \begin{Bmatrix} \mathbf{v}_1 \\ \mathbf{v}_2 \\ \mathbf{v}_3 \\ \mathbf{v}_4 \\ \mathbf{v}_5 \\ \mathbf{v}_6 \end{Bmatrix} \quad \text{where } \mathbf{v}_i = \begin{Bmatrix} w \\ w_{,x} \\ w_{,y} \\ w_{,xx} \\ w_{,xy} \\ w_{,yy} \end{Bmatrix}_i \quad \text{and } \mathbf{v}_j = \{w_{,n}\}_j \qquad \begin{matrix} i = 1, 2, 3 \\ j = 4, 5, 6 \end{matrix} \tag{27}$$

in which the indices $i$ and $j$ denote local nodal point numbers, see Figure 4. Equation (26) may be written as

$$\begin{Bmatrix} \mathbf{v}_1 \\ \mathbf{v}_2 \\ \mathbf{v}_3 \\ \mathbf{v}_4 \\ \mathbf{v}_5 \\ \mathbf{v}_6 \end{Bmatrix} = \begin{bmatrix} \mathbf{A}_1 \\ \mathbf{A}_2 \\ \mathbf{A}_3 \\ \mathbf{A}_4 \\ \mathbf{A}_5 \\ \mathbf{A}_6 \end{bmatrix} \mathbf{q}_{21} \tag{28}$$

The sub-matrices $\mathbf{A}_1$, $\mathbf{A}_2$ and $\mathbf{A}_3$ are found by introducing the coordinates of the corner nodes into the displacement functions and their appropriate derivatives. Hence

$$\mathbf{A}_i = \begin{bmatrix} 1 & x_i & y_i & x_i^2 & \dots & x_i^2 y_i^3 & x_i y_i^4 & y_i^5 \\ 0 & 1 & 0 & 2x_i & \dots & 2x_i y_i^3 & y_i^4 & 0 \\ 0 & 0 & 1 & 0 & \dots & 3x_i^2 y_i^2 & 4x_i y_i^3 & 5y_i^4 \\ 0 & 0 & 0 & 2 & \dots & 2y_i^3 & 0 & 0 \\ 0 & 0 & 0 & 0 & \dots & 6x_i y_i^2 & 4y_i^3 & 0 \\ 0 & 0 & 0 & 0 & \dots & 6x_i^2 y_i & 12x_i y_i^2 & 20y_i^3 \end{bmatrix} \tag{29}$$

where $i = 1, 2, 3$

In order to establish the three sub-matrices $\mathbf{A}_4$, $\mathbf{A}_5$ and $\mathbf{A}_6$ (row-matrices) an expression for the edge normal slope $w_{,n}$ must be found.

Consider first a rotation of the coordinate axes through an angle $\alpha$ about the $z$-axis, and let the new axes be denoted by $t$ and $n$ as shown in Figure 5.

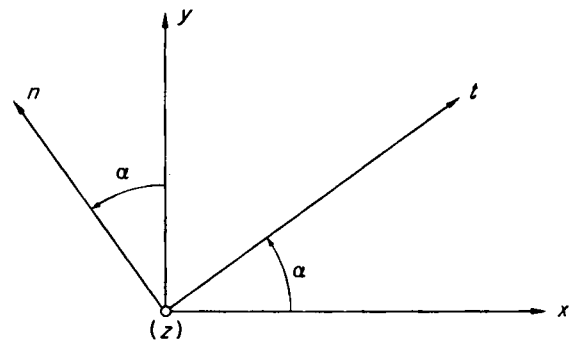


Figure 5. Rotation of axes

The relationship between the two systems may be expressed as

$$\left.\begin{aligned} t &= cx + sy \\ n &= -sx + cy \end{aligned}\right\} \quad \text{or} \quad \left\{\begin{aligned} x &= ct - sn \\ y &= st + cn \end{aligned}\right. \tag{30}$$

where the notation

$$\left.\begin{aligned} s &= \sin\alpha \\ c &= \cos\alpha \end{aligned}\right\} \tag{31}$$

has been introduced. Differentiation with respect to $t$ and $n$ gives

and

$$\left.\begin{aligned} \frac{\partial x}{\partial t} &= c \qquad \frac{\partial y}{\partial t} = s \\ \frac{\partial x}{\partial n} &= -s \qquad \frac{\partial y}{\partial n} = c \end{aligned}\right\} \tag{32}$$

Hence

$$\frac{\partial}{\partial t} = c\,\frac{\partial}{\partial x} + s\,\frac{\partial}{\partial y} \tag{33a}$$

and

$$\frac{\partial}{\partial n} = -s\,\frac{\partial}{\partial x} + c\,\frac{\partial}{\partial y} \tag{33b}$$

From these two equations it follows that

$$\begin{Bmatrix} \dfrac{\partial^2}{\partial t^2} \\ \dfrac{\partial^2}{\partial t \partial n} \\ \dfrac{\partial^2}{\partial n^2} \end{Bmatrix} = \begin{bmatrix} c^2 & 2sc & s^2 \\ -sc & c^2 - s^2 & sc \\ s^2 & -2sc & c^2 \end{bmatrix} \begin{Bmatrix} \dfrac{\partial^2}{\partial x^2} \\ \dfrac{\partial^2}{\partial x \partial y} \\ \dfrac{\partial^2}{\partial y^2} \end{Bmatrix} \tag{34}$$

Next, consider any one of the three sides of an arbitrary element. The axis normal to this side must be given a positive direction. With reference to Figure 6, positive direction of the axis $n_j$ ($j = 4, 5, 6$) is defined by

$$0 \leqq \beta_j < \pi$$

which implies that

$$0 \leqq \alpha_j < \frac{\pi}{2} \quad \text{or} \quad \frac{3\pi}{2} \leqq \alpha_j < 2\pi$$

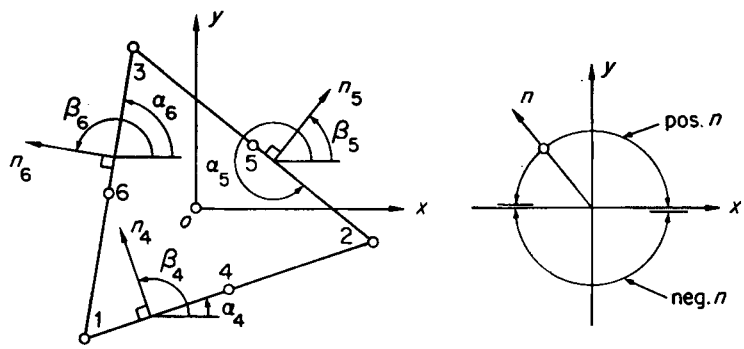


Figure 6. Angle notation and sign convention

The slope in the $n$-direction may, according to equation (33b), be expressed as

$$w_{,n} = -s\, w_{,x} + c\, w_{,y} \tag{35}$$

The last three sub-matrices of equation (28) are now easily determined. The transpose of $\mathbf{A}_j$ ($j = 4, 5, 6$) reads

$$\mathbf{A}_j^T = \begin{bmatrix} 0 \\ -s_j \\ c_j \\ -2s_jx_j \\ \vdots \\ 3c_jx_j^2y_j^2 - 2s_jx_jy_j^3 \\ 4c_jx_jy_j^3 - s_jy_j^4 \\ 5c_jy_j^4 \end{bmatrix} \tag{36}$$

where $s_j = \sin\alpha_j$, $c_j = \cos\alpha_j$ and $(x_j, y_j)$ are the coordinates of the mid-side nodes (see Figure 6).

With the transformation matrix $\mathbf{A}_{21}$ established the desired element stiffness matrix $\mathbf{k}_{21}$ is found by use of equations (11) and (10).

The element nodal forces $\mathbf{S}$ represent the actual loading on the element. In order to make these concentrated forces statically equivalent to a distributed transverse load $p(x,y)$ acting on the element, a virtual displacement field

$$\tilde{w}(x,y) = \boldsymbol{\phi}^T\tilde{\mathbf{q}} = \boldsymbol{\phi}^T\mathbf{B}\tilde{\mathbf{v}}$$

is imposed on the element. Equating the virtual work done by the distributed load $p(x,y)$ and the virtual work done by the equivalent concentrated nodal forces $\mathbf{S}$ during the virtual displacement gives

$$\mathbf{S}^T\tilde{\mathbf{v}} = \int_A p(x,y)\, \tilde{w}(x,y)\, \mathrm{d}A$$

$$= \int_A p(x,y)\, \boldsymbol{\phi}^T\, \mathrm{d}A\, \mathbf{B}\tilde{\mathbf{v}}$$

This equation is valid for any virtual displacement field. Hence

$$\mathbf{S} = \mathbf{B}^T\int_A p(x,y)\, \boldsymbol{\phi}\, \mathrm{d}A \tag{37}$$

or in terms of the 21 degree of freedom element

$$\mathbf{S}_{21} = \mathbf{B}_{21}^T\int_A p(x,y)\, \boldsymbol{\phi}_{21}\, \mathrm{d}A \tag{38}$$

A physical interpretation of the nodal forces is not called for and will not be attempted. It should be noted that the load $p(x,y)$ need not be uniformly distributed over the area. With the integration formulae in Table I it is also possible to treat a load having a hydrostatic distribution.

In general side nodes are undesirable. They have a severe disadvantage in that they cause a significant increase of the width of the band in the banded complete structure stiffness matrix. The side nodes, each of which is common to only two elements, also have a disproportionately large effect on the dimension of the complete structure stiffness matrix as compared to the corner nodes.

In the case of the 21 degree of freedom element, which will be designated T-21, only three degrees of freedom are associated with the mid-side nodes. A far more convenient 18 degree of freedom element, designated T-18, may therefore be obtained without much loss of refinement by eliminating the mid-side nodes of T-21. In order to maintain complete displacement and slope compatibility the mid-side nodes are eliminated by imposing a cubic variation on the normal slope $w_{,n}$ along the element edges. This is obtained by expressing $w_{,n}$ at the mid-side nodes in terms of the corner parameters.

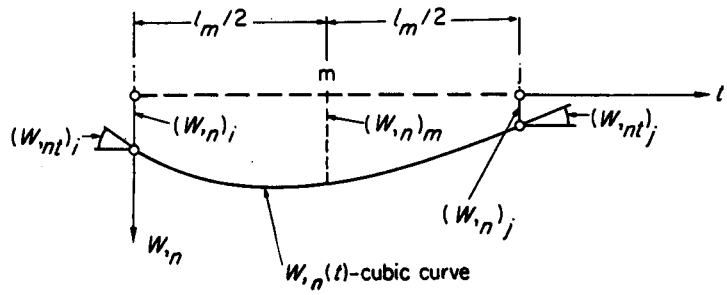


Figure 7. Variation of the normal slope along an arbitrary edge

The edge normal slope having a cubic variation along an arbitrarily oriented element edge $i$–$j$, as shown in Figure 7, may be expressed as

$$w_{,n}(t) = a_0 + a_1 t + a_2 t^2 + a_3 t^3 \tag{39}$$

Substituting the boundary conditions

$$\text{at } t = 0 \quad : \quad w_{,n} = (w_{,n})_i \text{ and } w_{,nt} = (w_{,nt})_i$$
$$\text{at } t = l_m \quad : \quad w_{,n} = (w_{,n})_j \text{ and } w_{,nt} = (w_{,nt})_j$$

into equation (39) yields

$$a_0 = (w_{,n})_i$$

$$a_1 = (w_{,nt})_i$$

$$a_2 = \frac{3}{l_m^2}\left[-(w_{,n})_i + (w_{,n})_j\right] - \frac{1}{l_m}\left[2(w_{,nt})_i + (w_{,nt})_j\right]$$

$$a_3 = \frac{2}{l_m^2}\left[(w_{,n})_i - (w_{,n})_j\right] + \frac{1}{l_m}\left[(w_{,nt})_i + (w_{,nt})_j\right]$$

Hence the normal slope at the mid-point '$m$' may be expressed as

$$(w_{,n})_m = \tfrac{1}{2}\left[(w_{,n})_i + (w_{,n})_j\right] + \frac{l_m}{8}\left[(w_{,nt})_i - (w_{,nt})_j\right] \tag{40}$$

The nodal parameters at the corner nodes are, however, expressed in a local global coordinate system $x,y$.

Let

$$\left.\begin{aligned} \kappa_1^{(m)} &= \tfrac{1}{2} s_m \\ \kappa_2^{(m)} &= \tfrac{1}{2} c_m \\ \kappa_3^{(m)} &= \tfrac{1}{8} l_m s_m c_m \\ \kappa_4^{(m)} &= \tfrac{1}{8} l_m (c_m^2 - s_m^2) \end{aligned}\right\} \tag{41}$$

where $s_m = \sin \alpha_m$ and $c_m = \cos \alpha_m$ (see Figure 6), and $l_m$ is the length of the element side on which node number $m$ lies ($m = 4, 5, 6$).

In the case of a cubically varying edge normal slope the value of $w_{,n}$ at the midside node '$m$' may now, by use of equations (40), (34), (35) and (41), be expressed in terms of the parameters at corner nodes '$i$' and '$j$' (local numbers) as

$$\begin{aligned} (w_{,n})_m = &- \kappa_1^{(m)}(w_{,x})_i + \kappa_2^{(m)}(w_{,y})_i - \kappa_1^{(m)}(w_{,x})_j + \kappa_2^{(m)}(w_{,y})_j \\ &- \kappa_3^{(m)}(w_{,xx})_i + \kappa_4^{(m)}(w_{,xy})_i + \kappa_3^{(m)}(w_{,yy})_i \\ &+ \kappa_3^{(m)}(w_{,xx})_j - \kappa_4^{(m)}(w_{,xy})_j - \kappa_3^{(m)}(w_{,yy})_j \end{aligned} \tag{42}$$

Positive direction of the axis $n$ is defined in Figure 6. Hence equation (42) is valid only if $x_j > x_i$. If $x_j < x_i$ the signs associated with the curvature terms must be changed.

The relationship between the side node parameters $\mathbf{v}_s$ and the corner node parameters $\mathbf{v}_c$ may be written as

$$\mathbf{v}_s = \mathbf{H}\mathbf{v}_c \tag{43}$$

in which

$$\mathbf{v}_s = \begin{Bmatrix} (w_{,n})_4 \\ (w_{,n})_5 \\ (w_{,n})_6 \end{Bmatrix} \quad \text{and} \quad \mathbf{v}_c = \begin{Bmatrix} \mathbf{v}_1 \\ \mathbf{v}_2 \\ \mathbf{v}_3 \end{Bmatrix} \tag{44}$$

where $\mathbf{v}_i$ ($i = 1, 2, 3$) is defined by equation (27).

The transformation matrix $\mathbf{H}$ may be expressed in partitioned form as

$$\mathbf{H} = \left[\mathbf{H}_1 \vdots \mathbf{H}_2 \vdots \mathbf{H}_3\right] \tag{45}$$

If $x_2 > x_3 > x_1$ then

$$\left.\begin{aligned}
\mathbf{H}_1 &= \begin{bmatrix} 0 & -\kappa_1^{(4)} & \kappa_2^{(4)} & -\kappa_3^{(4)} & \kappa_4^{(4)} & \kappa_3^{(4)} \\ 0 & 0 & 0 & 0 & 0 & 0 \\ 0 & -\kappa_1^{(6)} & \kappa_2^{(6)} & -\kappa_3^{(6)} & \kappa_4^{(6)} & \kappa_3^{(6)} \end{bmatrix} \\
\mathbf{H}_2 &= \begin{bmatrix} 0 & -\kappa_1^{(4)} & \kappa_2^{(4)} & \kappa_3^{(4)} & -\kappa_4^{(4)} & -\kappa_3^{(4)} \\ 0 & -\kappa_1^{(5)} & \kappa_2^{(5)} & \kappa_3^{(5)} & -\kappa_4^{(5)} & -\kappa_3^{(5)} \\ 0 & 0 & 0 & 0 & 0 & 0 \end{bmatrix} \\
\mathbf{H}_3 &= \begin{bmatrix} 0 & 0 & 0 & 0 & 0 & 0 \\ 0 & -\kappa_1^{(5)} & \kappa_2^{(5)} & -\kappa_3^{(5)} & \kappa_4^{(5)} & \kappa_3^{(5)} \\ 0 & -\kappa_1^{(6)} & \kappa_2^{(6)} & \kappa_3^{(6)} & -\kappa_4^{(6)} & -\kappa_3^{(6)} \end{bmatrix}
\end{aligned}\right\} \tag{46}$$

It should be noted that care must be taken in connection with the signs of the $\kappa_3^{(m)}$ and $\kappa_4^{(m)}$ terms. If for instance $x_1 = x_2$ the signs in equation (46) are correct only if $y_1 > y_2$. If $x_1 = x_2$ and $y_2 > y_1$ the signs associated with the $\kappa_3^{(4)}$ and $\kappa_4^{(4)}$ terms must be changed (see Figures 6 and 7 and equation 40).

For T-21 the element stiffness relation already established is

$$\mathbf{S}_{21} = \mathbf{k}_{21}\mathbf{v}_{21} \tag{47}$$

The corresponding element stiffness relation for T-18 is

$$\mathbf{S}_{18} = \mathbf{k}_{18}\mathbf{v}_{18} \tag{48}$$

in which

$$\mathbf{v}_{18} \equiv \mathbf{v}_c \tag{49}$$

The nodal forces $\mathbf{S}_{18}$ are defined in such a way that

$$\mathbf{S}_{18}^T\mathbf{v}_{18} = \mathbf{S}_{21}^T\mathbf{v}_{21} \tag{50}$$

From equations (43) and (49) it follows that in the case of the edge normal slope varying cubically along the element edges

$$\mathbf{v}_{21} \equiv \begin{Bmatrix} \mathbf{v}_c \\ \hline \mathbf{v}_s \end{Bmatrix} = \begin{bmatrix} \mathbf{I}_{18} \\ \hline \mathbf{H} \end{bmatrix} \mathbf{v}_{18} \tag{51}$$

Equations (50) and (51) imply that

$$\mathbf{k}_{18} = [\mathbf{I}_{18} \,\vdots\, \mathbf{H}^T]\, \mathbf{k}_{21} \begin{bmatrix} \mathbf{I}_{18} \\ \hline \mathbf{H} \end{bmatrix} \tag{52}$$

and

$$\mathbf{S}_{18} = [\mathbf{I}_{18} \,\vdots\, \mathbf{H}^T]\, \mathbf{S}_{21} \tag{53}$$

where $\mathbf{I}_{18}$ is the 18 by 18 identity matrix.

Alternatively $\mathbf{k}_{18}$ may be obtained directly from the generalized element stiffness matrix $\mathbf{k}_{q21}$. From equations (26) and (51) it follows that

$$\mathbf{A}_{21}\,\mathbf{q}_{21} = \begin{bmatrix} \mathbf{I}_{18} \\ \hline \mathbf{H} \end{bmatrix} \mathbf{v}_{18}$$

Hence

$$\mathbf{q}_{21} = \mathbf{A}_{21}^{-1}\left[\frac{\mathbf{I}_{18}}{\mathbf{H}}\right]\mathbf{v}_{18}$$

and

$$\mathbf{k}_{18} = \mathbf{G}^T\mathbf{k}_{q21}\mathbf{G} \tag{54}$$

in which

$$\mathbf{G} = \mathbf{A}_{21}^{-1}\left[\frac{\mathbf{I}_{18}}{\mathbf{H}}\right] \tag{55}$$

$\mathbf{k}_{18}$ is the element stiffness matrix for a fully compatible triangular plate bending element with nodal points at the corners only and with $3 \times 6 = 18$ nodal degrees of freedom.

The assembly process, i.e., the formation of the complete structure stiffness relation, and the application of the boundary conditions have been discussed extensively elsewhere,[2,14] and will not be dealt with here.

It should be noted that once the solution of the nodal displacement parameters has been obtained the internal moments at the nodal points may be determined directly by use of equation (1a).

## NUMERICAL RESULTS

Results obtained with a computer programme based on the refined 18 degree of freedom element (T-18) for two illustrative examples are presented below. In the first example results obtained with the 21 degree of freedom element (T-21) are included for comparison.

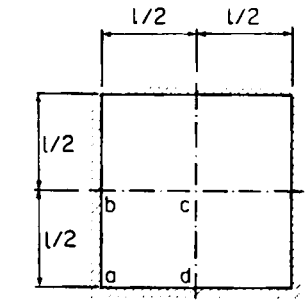


Poisson's ratio: $\nu = 0{\cdot}3$

| CASE | EDGES | LOAD |
|---|---|---|
| 1 | SS | U |
| 2 | SS | C |
| 3 | C | U |

EDGES: simply supported (SS) or clamped (C).

LOADING: uniform (U) or concentrated at centre (C).

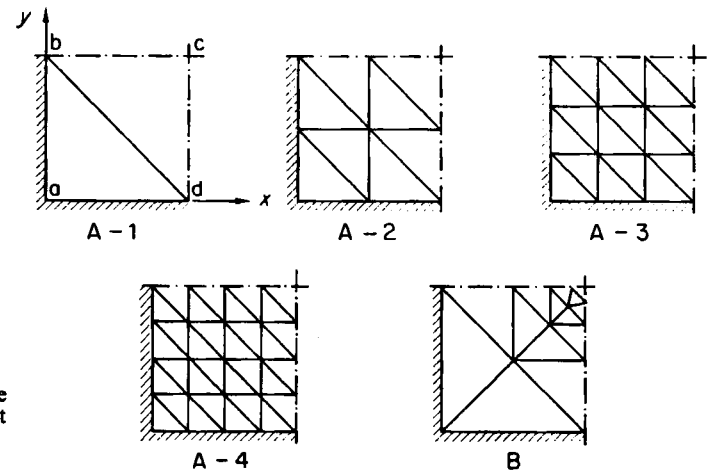


Figure 8. Schedule of square plate analysis and finite element idealizations

*Example* 1

Square plate of uniform thickness. Three combinations of support and loading conditions were considered:

Case 1. All edges simply supported—uniformly distributed load $p$.

Case 2. All edges simply supported—concentrated load $P$ at centre of plate.

Case 3. All edges clamped—uniformly distributed load $p$.

Poisson's ratio was taken to be $\nu = 0{\cdot}3$.

The plate geometry and the finite element idealizations are shown in Figure 8. Because of the double symmetry of the plate, only one quarter of it (a-b-c-d) was considered in the analysis.

Some representative values obtained with the refined elements T-18 and T-21 for deflection and internal moments, are shown in Tables II, III, and IV for Cases 1, 2, and 3 respectively. The analytical solutions shown in Table II (Case 1) were obtained by a computer programme based on a Navier solution, while those shown in Tables III and IV are given by Timoshenko.[10]

Table II. Square Plate Case 1

| Mesh | Deflection $w$ at centre (pt. c.) | | Bending moment $M_x = M_y$ at centre (pt. c) | | Twisting moment $M_{xy}$ at corner (pt. a) | |
|---|---|---|---|---|---|---|
| | T-18 | T-21 | T-18 | T-21 | T-18 | T-21 |
| A-1 | 4092 | 4057 | 4889 | 4916 | 3082 | 3167 |
| A-2 | 4063 | 4062 | 4791 | 4795 | 3204 | 3232 |
| A-3 | 4063 | 4062 | 4789 | 4790 | 3228 | 3241 |
| A-4 | 4062 | | 4788 | | 3236 | |
| Analytical solution | 4062 | | 4789 | | 3246 | |
| Multiplier | $10^{-6}\, pl^4/D$ | | $10^{-5}\, pl^2$ | | $-10^{-5}\, pl^2$ | |

Table III. Square Plate Case 2

| Mesh | Deflection $w$ at centre (pt. c) | | Twisting moment $M_{xy}$ at corner (pt. a) | |
|---|---|---|---|---|
| | T-18 | T-21 | T-18 | T-21 |
| A-1 | 1128 | 1138 | 6491 | 5904 |
| A-2 | 1153 | 1155 | 6152 | 6089 |
| A-3 | 1157 | 1158 | 6104 | 6093 |
| A-4 | 1158 | | 6097 | |
| B | 1160 | | 6081 | |
| Analytical solution | 1160 | | | |
| Multiplier | $10^{-5}\, Pl^2/D$ | | | $-10^{-5}\, P$ |

It is doubtful whether the analytical values in Table IV should be considered as exact values.

The results are largely self-explanatory. It is seen that the loss of accuracy resulting from the elimination of the midside nodes of T-21 is very small.

Table IV. Square Plate Case 3

| Mesh | Deflection $w$ at centre (pt. c) | | Bending moment $M_x = M_y$ at centre (pt. c) | | Bending moment $M_x$ at point $b$ ($M_y$ at point $d$) | |
|---|---|---|---|---|---|---|
| | T-18 | T-21 | T-18 | T-21 | T-18 | T-21 |
| A-1 | 114·9 | 124·6 | 225·7 | 265·7 | 392·6 | 567·9 |
| A-2 | 126·4 | 126·5 | 229·5 | 230·3 | 496·5 | 517·1 |
| A-3 | 126·5 | 126·5 | 229·1 | 229·3 | 510·2 | 513·9 |
| A-4 | 126·5 | | 229·1 | | 512·3 | |
| Analytical solution | 126 | | 231 | | 513 | |
| Multiplier | $10^{-5}\, pl^4/D$ | | $10^{-4}\, pl^2$ | | $-10^{-4}\, pl^2$ | |

*Example* 2

Equilateral triangular plate of uniform thickness. The plate is simply supported along all edges, and it carries a uniformly distributed load of intensity $p$. Poisson's ratio was again taken to be $\nu = 0{\cdot}3$.

The plate geometry and the finite element idealizations are shown in Figure 9. Because of the symmetry of the plate, only half of it was considered in the analysis.

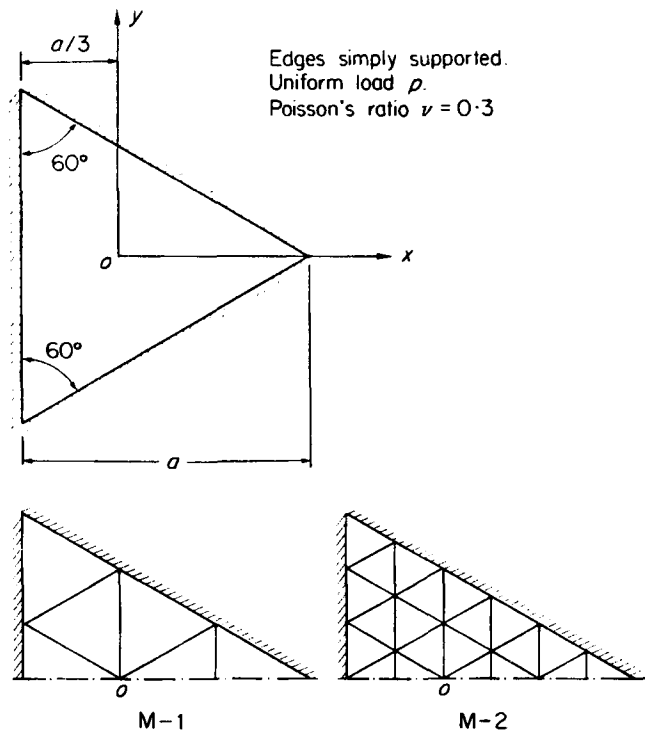


Figure 9. Plate geometry and finite element idealizations

Results obtained with the 18 degree of freedom element for the deflection and the bending moment ($M_x = M_y$) at the centre of gravity of the plate (point '$o$' in Figure 9) are shown in Table V compared with the analytical solution given by Timoshenko.[10]

Table V. Equilateral Triangular Plate Analysed by T-18

| Mesh | Deflection $w$ at point $o$ | Bending moment $M_x = M_y$ at point $o$ |
|---|---|---|
| M-1 | 10288 | 24068 |
| M-2 | 10288 | 24074 |
| Analytical solution | 10288 | 24074 |
| Multiplier | $10^{-7}\, pa^4/D$ | $10^{-6}\, pa^2$ |

From the results in Table V it is tempting to conclude that the analytical solution in this particular case must be contained in the finite element solution. This is, however, not the case. The analytical solution for the deflection as given in reference 10 reads

$$w = \frac{p}{64aD}\left[x^3 - 3y^2x - a(x^2 + y^2) + \frac{4}{27}a^3\right]\left(\frac{4}{9}a^2 - x^2 - y^2\right).$$

Examining this expression it is seen that the slope $w_x$, for example, describes a 4th order curve in the $y$-direction. In the finite element solution, however, a cubic variation has been imposed on the edge normal slope along all element boundaries. Theoretically speaking the two solutions are therefore not identical.

## CONCLUSIONS

The derivation of the stiffness matrix for a refined, fully compatible triangular plate bending finite element has been presented. Six nodal parameters or degrees of freedom have been introduced at each of three corner nodes, resulting in an 18 degree of freedom element.

Results obtained with this refined element show that it gives extremely good accuracy even for very coarse mesh idealizations. This is true for both deflection and stresses. Perhaps the most important feature of the refined element is the ease and accuracy with which it permits the internal moments to be determined. This is achieved by the introduction of the curvatures as nodal parameters. Another advantage obtained by having the curvatures among the nodal parameters is that they permit the boundary conditions to be satisfied more closely.

Very good convergence towards the correct solution is observed. In assessing the monotonic convergence it is important to recognize that it is the strain energy of the structure which should be examined. In Example 1, Case 2, the deflection under the concentrated load gives the strain energy, and Table III indicates a monotonic convergence (from the stiff side). A strict assessment of the monotonic convergence should omit the results obtained with meshes A-3 and B.

The derivation of the stiffness matrix follows standard procedures, and the development of very simple formulae for the integral of polynomial terms over the triangle area has made it possible to write explicit expressions for all elements of the generalized element stiffness matrix. However, the evaluation of the refined element stiffness matrix does require the inversion of a 21 by 21 transformation matrix, which is a straightforward but time-consuming operation on a digital computer. Although this inversion is a drawback, it does not appear to be a serious

one. In terms of computer time approximately 2·7 seconds are needed to evaluate the element stiffness matrix and the element nodal forces and to add them into the complete structure stiffness relation. This time refers to a FORTRAN IV programme on a UNIVAC-1107 computer.

ACKNOWLEDGMENTS

The work presented in this paper is based on the dissertation[14] submitted by the writer to the Department of Civil Engineering of the Technical University of Norway, in partial fulfillment of the requirements for the degree of Licentiatus Technicae. The investigation was made possible by a grant from the Technical University of Norway, and was conducted under the supervision of Professor I. Holand.

## APPENDIX

*Notation*

The following symbols are used in this paper:

1. *Scalars*

$A$ = area of triangle.
$a$ = plate dimension (Figure 9).
$a_i$ = constant (equation 39).
$c$ = abbreviation for cos $\alpha$.
$D$ = flexural rigidity of the plate.
$E$ = modulus of elasticity (Young's modulus).
$h$ = plate thickness.
$k$ = element of the stiffness matrix.
$l$ = plate dimension (Figure 8).
$l_m$ = length of element side $m$.
$M_x, M_y, M_{xy}$ = moment components in the $x$–$y$ system.
$n$ = direction normal to an element side.
$P$ = concentrated load.
$P_{rs}$ = $\int_A x^r y^s \, dA$,
$p$ = intensity of distributed transverse load.
$q$ = generalized displacement parameter.
$s$ = abbreviation for sin $\alpha$.
$t$ = direction of an element side.
$w$ = lateral displacement.
$x, y, z$ = Cartesian coordinates relative to centroid.
$\bar{x}, \bar{y}, \bar{z}$ = global Cartesian coordinates.
$\alpha, \beta$ = angles (Figure 6).
$\kappa$ = parameter defined by equation (41).
$\omega_1, \omega_2, \omega_3$ = area coordinates defined by equation (16).
$\rho$ = factor defined by equation (20).
$\nu$ = Poisson's ratio, and
$\phi_i$ = assumed displacement pattern.

2. *Vectors and Matrices*

$\mathbf{A}$ = transformation matrix defined by equation (8).

$\mathbf{B}$ = inverse of $\mathbf{A}$.

$\mathbf{c}$ = curvature vector defined by equation (4).

$\mathbf{D}$ = moment-curvature matrix defined by equation (1).

$\mathbf{G}$ = transformation matrix defined by equation (55).

$\mathbf{H}$ = transformation matrix defined by equation (43).

$\mathbf{I}$ = identity matrix.

$\mathbf{k}$ = element stiffness matrix.

$\mathbf{m}$ = moment vector defined by equation (1).

$\mathbf{P}$ = matrix defined by equation (4).

$\mathbf{Q}$ = generalized forces.

$\mathbf{q}$ = generalized displacement parameters.

$\mathbf{S}$ = element nodal forces.

$\mathbf{v}$ = element nodal displacement parameters, and

$\phi$ = vector containing assumed displacement functions.

## REFERENCES


1. M. J. Turner, R. W. Clough, H. C. Martin and L. J. Topp, 'Stiffness and deflection analysis of complex structures', *J. aeronaut. Sci.*, **23**, 9 (1956).
2. O. C. Zienkiewicz, *The Finite Element Method in Structural and Continuum Mechanics*, McGraw-Hill, London, 1967.
3. R. W. Clough and J. L. Tocher, 'Finite element stiffness matrices for analysis of plate bending', *Proc. Conf. Matrix Meth. Struct. Mech.*, Wright-Patterson Air Force Base, Dayton, Ohio (1965).
4. G. P. Bazeley, Y. K. Cheung, B. M. Irons and O. C. Zienkiewicz, 'Triangular elements in plate bending—conforming and nonconforming solutions', *Proc. Conf. Matrix Meth. Struct. Mech.*, Wright-Patterson Air Force Base, Dayton, Ohio (1965).
5. K. Hellan, 'Analysis of elastic plates in flexure by a simplified finite element method', *Acta polytech. scandi.*, Ci 46, Trondheim, Norway (1967).
6. L. R. Herrmann, 'Finite element bending analysis for plates', *J. Engng. Mech. Div. Am. Soc. civ. Engrs*, ASCE, 93 (1967).
7. H. Hansteen, 'Finite element displacement analysis of plate bending based on rectangular elements.' *International Symposium on the Use of Electronic Digital Computers in Structural Engineering*, Newcastle upon Tyne (1966).
8. C. A. Felippa, *Refined Finite Element Analysis of Linear and Nonlinear Two-Dimensional Structures*', SESM Report No. 66–22, University of California, Berkeley, California, 1966.
9. P. G. Bergan, *Plane Stress Analysis Using the Finite Element Method. Triangular Element with 6 Parameters in Each Node.* Division of Structural Mechanics, The Technical University of Norway, Trondheim, 1967.
10. S. Timoshenko and S. Woinowsky-Krieger, *Theory of Plates and Shells*, 2nd edn., McGraw-Hill, New York, 1959.
11. R. W. Clough, 'The finite element method in structural mechanics', in *Stress Analysis* (Ed. O. C. Zienkiewicz and G. S. Holister), Wiley, London, 1965, Chap. 7.
12. B. Fraeijs de Veubeke, 'Displacement and equilibrium models in the finite element method', in *Stress Analysis*, Chap. 9, cited above.[11]
13. R. G. Anderson, B. M. Irons and O. C. Zienkiewicz, *Vibration and Stability of Plates*, Research Report No. C/R/78/67, University of Wales, Swansea, 1967.
14. K. Bell, *Analysis of Thin Plates in Bending Using Triangular Finite Elements*, Division of Structural Mechanics, The Technical University of Norway, Trondheim, 1968.


Note—Since the acceptance of this paper the following publication, which deals with an element basically the same as the 21 degree of freedom element described in this paper, has come to our notice: 'Ein neues, vollverträgliches endliches Element für Plattenbiegung,' by W. Bosshard. Abhandlungen IVBH, Zürich, 1968, pp. 1–14.